

# Joint Bandwidth and Position Optimization in UAV Networks Deployed for Disaster Scenarios

**Abstract**—In this paper, we consider a disaster-affected area that has lost cellular connectivity. In such a scenario, we study a unmanned aerial vehicle (UAV) network deployed to restore the user connections to the core network. In particular, we propose a resource partitioning scheme for integrated access and backhaul in the downlink to sustain the user connections. First, we derive an analytical expression for the throughput coverage probability for the access (i.e., UAV to user) and the backhaul (i.e., terrestrial base station (BS) to UAV) links. Then, we investigate the optimal position of the UAV and the optimal partitioning of the frequency resources between the access and the backhaul links, in order to maximize the coverage of the users. Our study highlights that as the number of users in the network and/or their throughput demand increases, the optimal UAV position moves towards the centre of the disaster-affected area. Moreover, in that case, a higher fraction of the available frequency resources must be provisioned for the access links. On the contrary, when the backhaul throughput requirements are high, or in the case of sparsely deployed terrestrial BSs, the optimal UAV position is at the edge of the disaster-affected area. Thus, this study provides key system-design insights to a network operator for deploying emergency areal networks to extend the cellular coverage.

**Index Terms**—UAV Networks, Integrated Access and Backhaul, Resource Partitioning

## I. INTRODUCTION

In the past several years, with the growth of cellular traffic, the demand for seamless connectivity and coverage has increased. In order to sustain the quality of service (QoS) of the users, the telecom operators have adopted new strategies such as heterogeneous networks (HetNets) [1], cache-enabled UAVs [2] etc. The deployment of UAVs assist the terrestrial network of legacy BSs by temporarily increasing capacity and/or coverage in an ad-hoc manner. Further, in the case of emergency situations or disasters, the users in a particular area may loose connectivity to the cellular network due to the breakdown of the BSs. In such scenarios, UAVs acting as aerial BSs, can deliver reliable, cost-effective, and on-demand wireless communications to desired disaster effected areas [3]. Infact, their ability to adjust their altitude, will facilitate to enhance the likelihood of establishing a line-of-sight (LoS) communication link to the ground users, while maintaining a reliable backhaul connection to the terrestrial BSs.

For a successful transmission from the BSs to the users, the UAV locations need to be optimized. Additionally, an optimal distribution of the frequency resources between the access links and the backhaul link is necessary. However, due to limited bandwidth, power, etc, it becomes difficult to maintain these requirements in UAV networks [4]. Consequently, the design of integrated access and backhaul (IAB), by sharing the same spectral resources between the access and backhaul links, have gained popularity [5].

**Related work:** In [6], the authors have provided an overview of the opportunities and the challenges in deploying UAVs as BSs and as cellular-connected UAV-users. In [7], the effect of the urban propagation environment on the backhaul links of the UAV network and the coverage probability experienced by the end user is investigated. In [8], the authors have derived the signal to interference noise ratio (SINR)  $k$ -coverage probability experienced by the user for downlink channel. They have derived expression for distribution of the SINR experienced by a typical user in the downlink channel from the  $k$ -th strongest base stations of a cellular network. A similar work is presented in [9], where the authors have described the fundamentals of modelling a network using binomial point process (BPP) and have investigated the coverage performance of a single UAV-network by considering two policies. In the first policy, the serving user is chosen randomly, whereas, in the second, the serving user is assumed to be the  $k$ -th closest node to the UAV. However, the authors have not considered any backhaul constraints in the system.

IAB in UAVs is explained as a latent solution for flexible and vast deployment of 5G New Radio (5G NR) without densifying the current terrestrial infrastructure [10]. The authors in [11], have presented a model for forward link transmissions in an integrated access and backhaul cellular network by utilizing the flying capability of UAVs. The authors in [12], have proposed a backhaul-limited optimal UAV-BS placement algorithm and have studied the effect of the users' mobility on the UAV placement. In [13] the authors have introduced a trade-off factor for resource allocation in order to improve the performance of UAV enabled networks with wireless backhaul. Based on the achievable rate, they have formulated a resource allocation problem to improve the users data rate.

As evident from the above, none of the existing researchers have explored joint optimization of the bandwidth allocation and the UAV placement to maximize user coverage in a disaster affected area. Motivated by the above, in this paper, we analyze the the trade-off in allocating the frequency resources between access and backhaul links, while optimizing the UAV location. Our method is based on a bandwidth allocation factor  $\beta$  for dividing frequency resources between access and backhaul links, which we optimize jointly with the UAV position  $u_0$ . The main contributions of the paper are as follows.

- We perform a stochastic geometry based downlink signal to noise ratio (SNR) coverage analysis of a wireless network consisting of a UAV deployed in a disaster struck area. The UAV provides wireless access to the users in the area, while connected to the nearest terrestrial BS outside the disaster-affected area for wireless backhaul. We derive the distance distribution of the users in access link (UAV to user) and the nearest BS in the backhaul

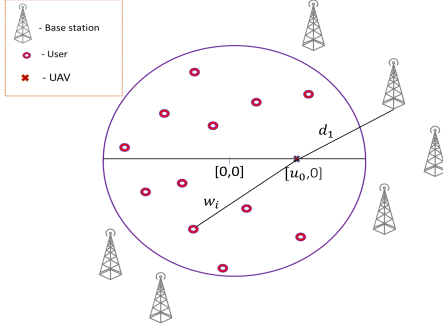


Fig. 1: System model.

link (BS to UAV).

- Leveraging on the distance distributions, we derive an analytical expression for the throughput coverage probability of the users by taking into account both the access and the backhaul links. Then, we investigate the optimal value of  $\beta$  and optimal  $u_0$  in order to maximize the throughput coverage probability of the system.
- The joint optimization of  $\beta$  and  $u_0$  is non-trivial in general due to their inter-dependence. As a first study, we provide the trends of the optimal  $\beta$  and  $u_0$  for varying number of users, access and backhaul throughput thresholds, and BS densities. Our study provides key system-design insights for deploying UAV networks for coverage extension in disaster-affected areas.

## II. SYSTEM MODEL

We consider a disaster-affected area, modeled as a circle  $A = \mathcal{B}(0, r_d)$  with origin as the center, and a radius  $r_d$  in the two-dimensional Euclidean plane. We assume that inside the circle, the users have lost cellular connectivity due to the breakdown of BSs. Thus, all terrestrial BSs are located in  $\mathbb{R}^2 \setminus A$ . In this scenario, we consider a downlink network consisting of a single UAV located in  $A$  providing coverage to the users. Furthermore, the UAV is connected to the nearest BS for backhaul communication. The overall scenario is depicted in Fig. 1. We analyze the performance of the downlink system with respect to a fixed number of users  $N_u$ , which are randomly located in  $A$  and request critical information from the cellular network for emergency response. In particular, the location of the users are modelled as points of a BPP in  $A$ . The macro BSs are modelled as points of homogeneous poisson point process (PPP),  $\Phi_t$  with intensity  $\lambda_t$ , in  $\mathbb{R}^2 \setminus A$ . The 2D position of the UAV is restricted inside  $A$ . The UAV is located at a position  $\mathbf{r}_0$ . Due to the rotation invariance of BPP, we align the x-axis along the direction of the UAV [9] such that  $\mathbf{r}_0 = (u_0, 0)$ , where  $u_0 = \|\mathbf{r}_0\| \in [0, r_d]$ .

We partition the total available bandwidth  $B$  between the access and the backhaul links using the factor  $\beta$ . Thus, the combined allotted bandwidth to the access link is  $\beta B$  and the bandwidth allotted to the backhaul link is  $(1 - \beta)B$ . Further, for the access link, we use orthogonal frequency allocation to the users. Since, we consider a disaster scenario, we assume that the BSs outside the affected area are sparse, thus, the interference from other BSs is limited. However, the impact

of interference can be easily integrated in our study, which we will treat in a future work. The transmit powers of UAV and the BS are denoted as  $P_u$  and  $P_t$ , respectively. As the paper focuses on the study of the resource partitioning trade-off between access and backhaul links, we consider a simple channel model which can be extended to a more generic model in future. The access and backhaul links are characterized by a small-scale Rayleigh fading  $h$ , the power of which follows an exponential distribution with unit mean. The power received at the  $i^{\text{th}}$  user from the UAV is  $P_{ra} = P_u K w_i^{-\alpha} h_1$  where  $w_i$  is the planar distance separating the  $i^{\text{th}}$  user and the UAV,  $K$  is the path-loss coefficient, i.e.,  $K = (\frac{\lambda_c}{4\pi})^2$ , where  $\lambda_c$  is the carrier wavelength. The parameter  $\alpha$  is the path-loss exponent and  $h_1$  is the fading in the access link. The received power at the UAV from the nearest BS for backhaul is given as  $P_{rb} = P_t K d_1^{-\alpha} h_2$  where  $d_1$  is distance of the nearest BS from the UAV and  $h_2$  is the fading in the backhaul link.

The metric of interest in our study is the system throughput coverage probability ( $R$ ), defined as the product of throughput coverage probability of the access link and the backhaul link. Ergodically, it represents the fraction of successful transmissions from the BS to the user via the UAV.

## III. CHARACTERIZATION OF THROUGHPUT COVERAGE PROBABILITY

In order to study the system throughput coverage probability, let us characterize the throughput coverage probability of access link and backhaul links.

**Lemma 1.** *The throughput coverage probability of the access link is given as*

$$R_a(\gamma_a, u_0) = \int_0^{r_d - u_0} R_{a1} f_{1a}(w_i | u_0) d(w_i) + \int_{r_d - u_0}^{r_d + u_0} R_{a1} f_{2a}(w_i | u_0) d(w_i), \quad (1)$$

where,  $R_{a1} = \exp\left[-\left\{\frac{N_p}{P_u K w_i^{-\alpha}} \left(2^{\frac{N_u \gamma_a}{\beta B}} - 1\right)\right\}\right]$  and  $f_{1a}(w_i | u_0)$  and  $f_{2a}(w_i | u_0)$  are the distance distribution of the users in access link.

$$f_a(w_i | u_0) = \begin{cases} f_{1a}(w_i | u_0) & 0 \leq w_i \leq r_d - u_0 \\ f_{2a}(w_i | u_0) & r_d - u_0 \leq w_i \leq r_d + u_0, \end{cases} \quad (2)$$

where,

$$f_{1a}(w_i | u_0) = 2w_i / r_d^2, \quad (3)$$

$$f_{2a}(w_i | u_0) = \frac{2w_i}{\pi r_d^2} \cos^{-1}\left(\frac{-r_d^2 + w_i^2 + u_0^2}{2u_0 w_i}\right). \quad (4)$$

*Proof:* The throughput for access link is given as

$$R_u = \beta \left(\frac{B}{N_u}\right) \log_2(1 + SNR_a),$$

where,  $SNR_a$  is the SNR of the access link.  $SNR_a = \frac{P_{ra}}{N_p}$ , where  $N_p$  is the additive white gaussian noise (AWGN) power. To characterize this, we need to first derive the distance distribution of the users from the UAV.

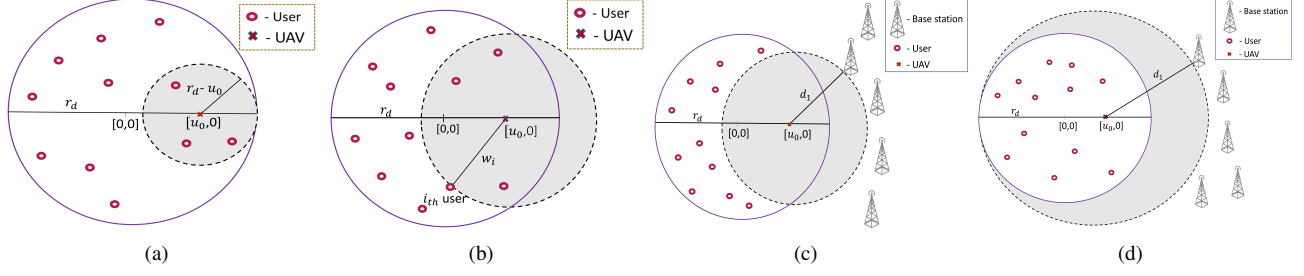


Fig. 2: (a) Access link- Users close to the UAV (b) Access link- Users far from the UAV (c) Backhaul link- Nearest BS close to the circle of radius  $r_d$  (d) Backhaul link- Nearest BS far from the circle of radius  $r_d$

The conditional cumulative distribution function (CDF) of a typical user located at a distance of  $w_i$  from  $u_0$  is [9]:

$$F_a(w_i|u_0) = \begin{cases} F_{1a}(w_i|u_0), & 0 \leq w_i \leq r_d - u_0 \\ F_{2a}(w_i|u_0), & r_d - u_0 \leq w_i \leq r_d + u_0. \end{cases} \quad (5)$$

Without loss of generality, let us assume that the UAV lies at the positive side of the x-axis. The CDF of  $w_i$  is derived using the geometric argument applied in [14, Th. 2.3.6]. There are two cases: i)  $w_i \leq r_d - u_0$ , i.e., when the circle with a radius joining the UAV and the user is completely inside the outer circle as in Fig. 2(a), and ii)  $w_i > r_d - u_0$ , i.e., when the users are far enough from the UAV position such that the intersection area is not entirely inside the circle of radius  $r_d$  as in Fig. 2(b).

For the first case, the CDF is simply:

$$F_{1a}(w_i|u_0) = w_i^2 / r_d^2.$$

For the second case, we compute the intersection area of the circles of radius  $r_d$  and  $w_i$  to compute the CDF of a user at a distance of  $w_1$  from  $u_0$ . As the users are distributed as BPP, the CDF for a given user located outside the circle of radius  $(r_d - u_0)$  which is at a distance of  $w_1$  from  $u_0$  is given as

$$F_{2a}(w_i|u_0) = \frac{w_i^2}{\pi r_d^2} \left[ w_i^2 \left( \theta - \frac{1}{2} \sin 2\theta \right) + r_d^2 \left( \phi - \frac{1}{2} \sin 2\phi \right) \right]$$

where,  $\theta = \cos^{-1} \left( \frac{-r_d^2 + w_i^2 + u_0^2}{2u_0 w_i} \right)$  and  $\phi = \cos^{-1} \left( \frac{r_d^2 - w_i^2 + u_0^2}{2u_0 r_d} \right)$ .

The conditional probability density function (PDF) of  $w_i$  for a given  $u_0$  is obtained by taking the derivative of CDF with respect to  $w_i$  as given in Lemma 1, (2).

The throughput coverage probability of access link is obtained by comparing the rate throughput with  $\gamma_a$ , i.e.,  $\mathbb{P}(R_u > \gamma_a)$  where,  $\gamma_a$  is the throughput threshold defined for access link. The throughput coverage probability of access link is

$$R_a = \int \left( \exp \left[ \left\{ \frac{-N_p}{P_u K w_i^{-\alpha}} \left( 2^{\frac{N_u \gamma_a}{B\beta}} - 1 \right) \right\} \right] \right) f_a(w_i|u_0) dw_i.$$

$$R_a = \int_0^{r_d - u_0} R_{a1} f_{1a}(w_i|u_0) d(w_i) + \int_{r_d - u_0}^{r_d + u_0} R_{a1} f_{2a}(w_i|u_0) d(w_i), \quad (6)$$

**Lemma 2.** The throughput coverage probability for the backhaul link is given as

$$R_b(\gamma_b, u_0) = \int_{r_d - u_0}^{R_2} R_{b1} f_{d1}(d_1|u_0) d(d_1), \quad (7)$$

where,  $R_{b1} = \exp \left[ - \left\{ \frac{N_p}{P_t K d_1^{-\alpha}} \left( 2^{\frac{\gamma_b}{B(1-\beta)}} - 1 \right) \right\} \right]$  and  $f_{d1}(d_1|u_0)$  is distance distribution of the nearest BS.

$$f_b(d_1|u_0) = \begin{cases} f_{1b}(d_1|u_0) & \text{if } -r_d < x_0 < r_d \\ f_{2b}(d_1|u_0) & \text{if } x_0 \leq -r_d. \end{cases} \quad (8)$$

where,  $f_{1b}(d_1|u_0)$  is given in (11) and

$$f_{2b}(d_1|u_0) = 2\pi d_1 \lambda_t \exp \left( - \lambda_t (\pi d_1^2 - \pi r_d^2) \right). \quad (9)$$

*Proof:* The rate throughput for backhaul link is given as

$$R_t = (1 - \beta) B \log_2(1 + SNR_b),$$

where,  $SNR_b = \frac{P_{rb}}{N_p}$ . Similar to the access, there are two conditions: i)  $-r_d < x_0 < r_d$  and ii)  $x_0 \leq -r_d$ . We compute the intersection area of the circles in Fig. 2(c), to find the CDF of the nearest BS which is at a distance of  $d_1$  from  $u_0$ .

1)  $-r_d < x_0 < r_d$ :  $x_0$  is the projection of the point of intersection of two circles on x-axis.

Since, the BSs are outside the circle of radius  $r_d$  and they are distributed as PPP, the conditional CDF of the nearest BS located at a distance  $d_1$  from  $u_0$  is given as

$$F_{1b}(d_1|u_0) = 1 - \exp \left( - \lambda_t \left( d_1^2 \left( \pi/2 + y \sqrt{1 - y^2} - \tan^{-1} \frac{-y}{\sqrt{1 - y^2}} \right) - r_d^2 \left( \pi/2 - x \sqrt{1 - x^2} - \tan^{-1} \frac{x}{\sqrt{1 - x^2}} \right) \right) \right), \quad (10)$$

where,  $x = \frac{r_d^2 - d_1^2 + u_0^2}{2u_0 r_d}$  and  $y = \frac{u_0^2 - r_d^2 + d_1^2}{2u_0 d_1}$ .

To find the PDF of  $d_1$ , the derivative of CDF is computed. The conditional PDF of  $d_1$  for a given  $u_0$ ,  $f_{1b}(d_1|u_0)$  is given in (11), where  $z = \frac{d_1^2 + r_d^2 - u_0^2}{2u_0 d_1^2}$ .

TABLE I: Simulation Parameters

Notation	Parameter	Value
$r_d$	Radius of circle in which users exist	100 m
$N_u$	Number of users	15-30
$\lambda_t$	Intensity of BSs	$1 \text{ Km}^{-2}$
$B$	Bandwidth of the system	20 MHz
$\alpha$	Path-loss Exponent	2
$f$	Carrier frequency	2 Ghz
$P_u$	Power for Access link	10 dBm
$P_t$	Power for Backhaul link	20 dBm
$\gamma_a$	Access Throughput Threshold	10 Mbps
$\gamma_b$	Backhaul Throughput Threshold	200 Mbps
$K$	Path-loss Coefficient	$1.5e-4$

2)  $x_0 \leq -r_d$ : In Fig. 2(d), the intersection area of two circles is the area of the circle with radius  $r_d$  itself. So, the CDF of the distance of nearest BS  $d_1$  from  $u_0$  is

$$F_{2b}(d_1|u_0) = 1 - \exp\left(-\lambda_t(\pi d_1^2 - \pi r_d^2)\right). \quad (12)$$

The conditional PDF of  $d_1$  with respect to  $u_0$ ,  $f_{2b}(d_1|u_0)$  is given in Lemma 2, (9).

The throughput coverage probability of backhaul link is obtained by comparing the rate throughput with  $\gamma_b$  i.e.,  $\mathbb{P}(R_t > \gamma_b)$  where,  $\gamma_b$  is the throughput threshold for the backhaul link. Therefore, the throughput coverage probability for the backhaul link is given as

$$R_b(\gamma_b, u_0) = \int_{r_d - u_0}^{R_2} R_b f_b(d_1|u_0) d(d_1), \quad (13)$$

$R_2$  is the upper limit for the area in which BSs are present. ■

We conclude from (6) that  $R_a$  is higher for smaller values of  $u_0$  i.e., when the UAV is at the center of the circle in which users are present and increases as  $\beta$  increases. And, from (13),  $R_b$  is higher for larger values of  $u_0$  i.e., when UAV is at the edge of the circle and decreases as  $\beta$  increases.

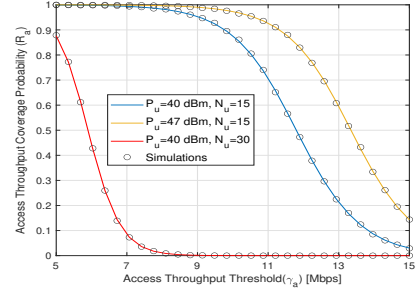
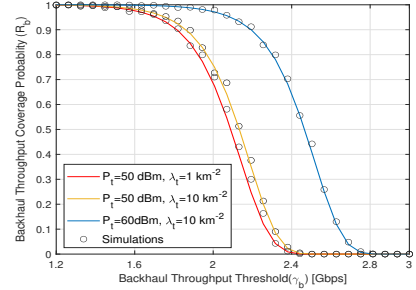
Therefore, the success probability of the whole system has a combined effect of throughput coverage probability of access and backhaul links and is calculated as follows

$$R(\gamma_a, \gamma_b, u_0) \approx R_a(\gamma_a, u_0) \cdot R_b(\gamma_b, u_0). \quad (14)$$

#### IV. RESULTS AND DISCUSSIONS

This section presents the results obtained from our analytical observations and validated through Monte-Carlo simulations. The simulation parameters are shown in Table I. In Fig. 3, we plot the throughput coverage probability for the access link ( $R_a$ ), with respect to  $\gamma_a$ . As  $\gamma_a$  or  $N_u$  increases,  $R_a$  decreases. This is because, as more users access the network, total throughput requirement increases, thus  $R_a$  decreases. The good agreement between the simulated and the theoretical expressions validates the derived analytical framework.

In Fig. 4, we plot the throughput coverage probability for the backhaul link ( $R_b$ ) with respect to  $\gamma_b$ . The throughput coverage probability decreases with an increase in the backhaul throughput threshold. Furthermore, as  $P_t$  increases, the value of  $R_b$  increases because the probability of the nearest BS in the backhaul to get covered increases as backhaul power increases. Further, as  $\lambda_t$  increases,  $R_b$  increases for the same value of


 Fig. 3: Trends in  $R_a$  against  $\gamma_a$  for different  $P_u$  and  $N_u$ 

 Fig. 4: Trends in  $R_b$  against  $\gamma_b$  for different  $P_t$  and  $\lambda_t$ 

$P_t$ . Because, as  $\lambda_t$  increases, the distance of the nearest BS from the UAV decreases, so  $R_b$  increases.

Therefore, as the rate requirement of users in the access link increases, the backhaul capacity is affected which can be compensated by decreasing the backhaul throughput threshold.

**Throughput Coverage Probability:** Figs. 5(a) and 5(b) show the variation of throughput coverage probability with respect to  $\beta$  by varying access and backhaul system parameters respectively. In Fig. 5(a), since for smaller values of  $\beta$ , the bandwidth allocated to access link is less compared to the backhaul link, the overall coverage is limited. On the contrary, for higher values of  $\beta$ , the bandwidth allocated to backhaul is decreases, which also limits the overall coverage. Thus, the overall throughput coverage probability of the whole system increases as  $\beta$  increases, reaches its peak for a particular value of  $\beta$ , and decreases after that. Furthermore, as  $\gamma_a$  increases, the throughput requirement for the access link increases, thus the optimal  $\beta$  increases. Similarly, as  $N_u$  increases, in order to meet the throughput requirements of more users, more fraction of bandwidth is allocated to the access link. We observe an opposite trend for  $\beta$  in Fig. 5(b). In particular, when  $\gamma_b$  or  $\lambda_t$  increases, the throughput requirement for the backhaul link increases, and hence, the optimal value for  $\beta$  decreases to provide more bandwidth  $((1 - \beta)B)$  to the backhaul link.

Figs. 5(c) and 5(d) show the variation of throughput coverage probability with respect to  $u_0$  by varying access and backhaul system parameters respectively. From Fig. 5(c), for smaller values of  $u_0$ ,  $R_b$  is less when compared to  $R_a$ . This is because, UAV is located towards the center of the circle and throughput coverage probability of backhaul link,  $R_b$  decreases. And for higher values of  $u_0$ ,  $R_a$  is less when compared to  $R_b$ . This is because, UAV is located at the

$$f_{1b}(d_1|u_0) = \lambda_t \exp\left(-\lambda_t \left(d_1^2 \left(\frac{\pi}{2} + y\sqrt{1-y^2} - \tan^{-1} \frac{-y}{\sqrt{1-y^2}}\right) - r_d^2 \left(\frac{\pi}{2} - x\sqrt{1-x^2} - \tan^{-1} \frac{x}{\sqrt{1-x^2}}\right)\right)\right) \times \frac{-d_1 r_d}{u_0} \left[2\sqrt{1-x^2}\right] + z d_1^2 \left[2\sqrt{1-y^2}\right] + 2d_1 \left[y\sqrt{1-y^2} + \frac{\pi}{2} - \tan^{-1} \frac{-y}{\sqrt{1-y^2}}\right] \quad (11)$$

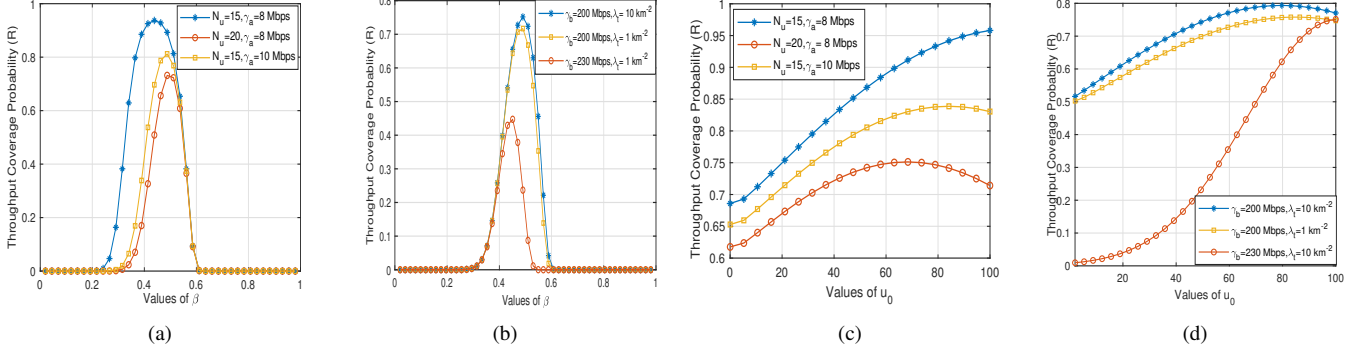


Fig. 5: Trends in throughput coverage probability with respect to (a)  $\beta$  for different values of  $N_u$  and  $\gamma_a$  (b)  $\beta$  for different values of  $\gamma_b$  and  $\lambda_t$  (c)  $u_0$  for different values of  $N_u$  and  $\gamma_a$  (d)  $u_0$  for different values of  $\gamma_b$  and  $\lambda_t$

edge of the circle and throughput coverage probability of access,  $R_a$  decreases. Thus, there exists an optimal value of  $u_0$  that maximizes the system throughput coverage probability.

Furthermore, when the value of  $\gamma_a$  or  $N_u$  increases, the throughput requirement for the access link increases, and accordingly, the UAV shifts towards the center of the circle of radius  $r_d$  to meet the throughput requirement of the users in access link. Nevertheless, in Fig. 5(d), as  $\gamma_b$  or  $\lambda_t$  increases, the throughput requirement for the backhaul link increases and hence, the UAV shifts to the edge in order to provide more coverage to the nearest BS in the backhaul link.

**Optimum  $\beta$  and Optimum  $u_0$ :** In Fig. 6(a), we plot the variation of optimal values of  $\beta$  and optimal throughput coverage probability ( $R$ ) with respect to  $\gamma_a$  for a fixed value of  $u_0$ . As  $\gamma_a$  increases, in order to cater for the high throughput requirement of the access link, the optimal value of  $\beta$  also increases. Further, because of a decrease in  $R_a$ , the optimal throughput coverage probability of the system also decreases as  $\gamma_a$  increases. For a specific value of  $\gamma_a$ , as  $P_u$  increases, the throughput requirement for the access link decreases, so the value of optimal  $\beta$  decreases and the optimal throughput coverage probability  $R$  increases. As  $N_u$  increases, for a specific value of  $\gamma_a$ , the throughput requirement of the access link increases. In order to support the increased throughput requirement, the value of optimal  $\beta$  increases and  $R$  decreases. Fig. 6(b) shows the variation of optimal values of  $\beta$  and  $R$  with respect to  $\gamma_b$  for a fixed  $u_0$ . As  $\gamma_b$  increases, to cater for the high throughput requirement of the backhaul link, the optimal value of  $\beta$  decreases. Further, the optimal coverage probability decreases with the increase in  $\gamma_b$  because of decrease in  $R_b$ . For a specific value of  $\gamma_b$ , as  $P_t$  increases, the throughput requirement for the backhaul link decreases, so the value of optimal  $\beta$  increases and the optimal throughput coverage probability  $R$  increases. As  $\lambda_t$  decreases, for a specific value of  $\gamma_b$ , the distance of nearest BS from the UAV increases

and therefore, the throughput requirement of the backhaul link increases. In order to cater for this, the value of optimal  $\beta$  and  $R$  decrease as  $\gamma_b$  increases. Fig. 6(c) shows the variation of optimal values of  $\beta$  and  $R$  with respect to  $N_u$  for a fixed  $u_0$ . As  $N_u$  increases, to cater for the increased throughput requirement of the access link the optimal value of  $\beta$  also increases. Further, because of a decrease in  $R_a$ , the optimal throughput coverage probability for the system also decreases. For a specific value of  $N_u$ , as  $P_u$  increases, the throughput requirement for the access link decreases, so the value of optimal  $\beta$  decreases and the optimal throughput coverage probability increases. As  $\gamma_a$  increases, for a specific value of  $N_u$ , the access throughput requirement increases. In order to cater for this, the value of optimal  $\beta$  increases and  $R$  decreases.

In Fig. 7(a), we plot the variation of optimal values of  $u_0$  and optimal throughput coverage probability ( $R$ ) with respect to  $\gamma_a$  for a fixed  $\beta$ . As  $\gamma_a$  increases, the throughput requirement of access link increases, and to meet the requirement of access link, the UAV shifts towards the center of the circle of radius  $r_d$ . Further, as  $\gamma_a$  increases, the optimal throughput coverage probability decreases. For a specific value of  $\gamma_a$ , as  $P_u$  increases, the throughput requirement for the access link decreases and the UAV shifts towards the edge in order to maintain the throughput coverage. Also, as  $N_u$  increases, for a specific value of  $\gamma_a$ , the throughput requirement of the access link increases and the optimal value of  $u_0$  and  $R$  decrease. Fig. 7(b), shows the variation of optimal values of  $u_0$  and  $R$  with respect to  $\gamma_b$  for a fixed  $\beta$ . As  $\gamma_b$  increases, the throughput requirement of backhaul link increases, so the UAV shifts towards the edge of the circle. Further, as  $\gamma_b$  increases,  $R_b$  decreases which leads to a decrease in the optimal throughput coverage probability. For a specific value of  $\gamma_b$ , as  $P_t$  increases, the throughput requirement for the backhaul link decreases and the UAV shifts towards the center in order to maintain the throughput coverage probability. Also,



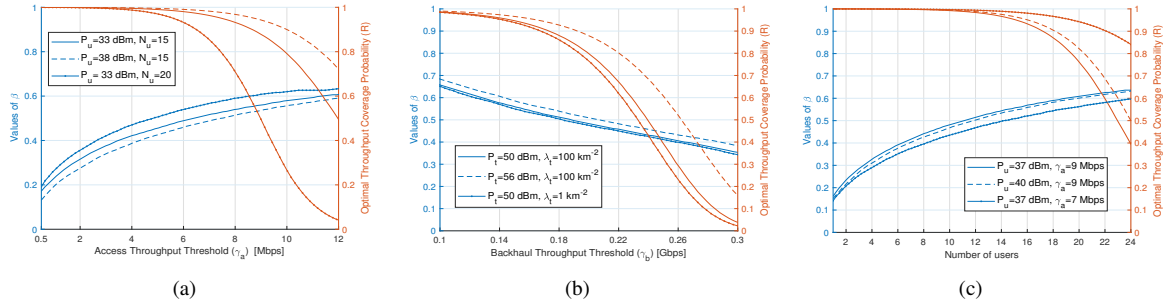


Fig. 6: Variation of optimal  $\beta$  with respect to a)  $\gamma_a$ , b)  $\gamma_b$ , and c)  $N_u$ .

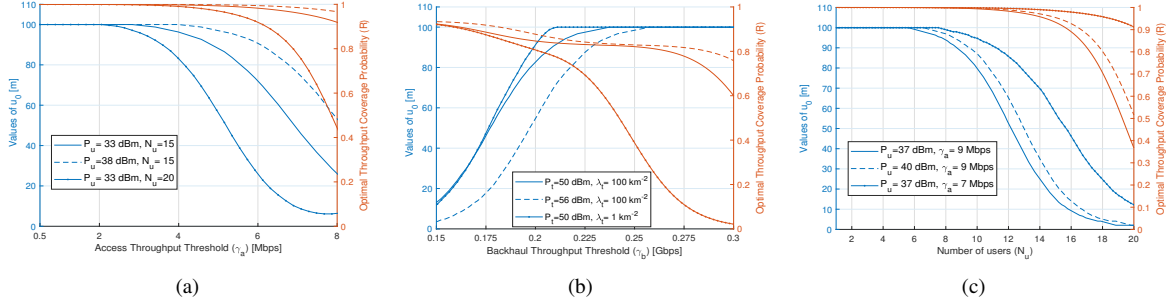


Fig. 7: Variation of optimal  $u_0$  with respect to a)  $\gamma_a$ , b)  $\gamma_b$ , and c)  $N_u$ .

as  $\lambda_t$  decreases, for a specific value of  $\gamma_b$ , the throughput requirement of the backhaul link increases, as the distance of UAV to the nearest BS increases. Therefore, the optimal value of  $u_0$  increases and  $R$  decrease. Fig. 7(c) shows the variation of optimal values of  $u_0$  and  $R$  with respect to  $N_u$  for a fixed  $\beta$ . As  $N_u$  increases, the throughput requirement of access link increases, and the UAV shifts towards the center of the circle of radius  $r_d$  to meet the throughput demand. As  $N_u$  increases, there is a decrease in the the optimal throughput coverage probability. Further, for a specific value of  $N_u$ , as  $P_u$  increases, the throughput requirement for the access link decreases and the UAV shifts away from the center in order to maintain the throughput coverage. As  $\gamma_a$  increases, the throughput requirement of the access link increases and the optimal value of  $u_0$  and  $R$  decrease.

## V. CONCLUSION

In this paper, we have characterized a downlink single UAV network using stochastic geometry, to analyze the performance of access link (UAV to user) and backhaul link (BS to UAV) by characterizing throughput coverage probability of the system. The expression for optimal overall throughput coverage probability of the system by taking the trade-off factor ( $\beta$ ) and planar position of UAV ( $u_0$ ) as our key parameters is derived. As a possible extension, a joint optimization of  $\beta$  and  $u_0$  by taking into account the effect of interference from both access and backhaul links can be performed, however that will be a subject of future work.

## REFERENCES

[1] Y. J. Chun, M. Hasna, and A. Ghrayeb, "Modeling heterogeneous cellular networks interference using poisson cluster processes," *IEEE*

*Journal on Selected Areas in Communications*, vol. 33, pp. 1–1, 10 2015.

[2] N. Z. Y. C. J. T. F. Cheng, G. Gui and H. Sari, "UAV-relaying-assisted secure transmission with caching," *IEEE Transactions on Communications*, vol. 67, pp. 3140–3153, 5 2019.

[3] M. Erdelj and E. Natalizio, "UAV-assisted disaster management: Applications and open issues," 02 2016, pp. 1–5.

[4] J. Li and Y. Han, "Optimal resource allocation for packet delay minimization in multi-layer UAV networks," *IEEE Communications Letters*, vol. 21, pp. 580–583, 3 2017.

[5] N. T. et al, "Aerial access and backhaul in mmwave B5G systems: Performance dynamics and optimization," *IEEE Communications Magazine*, vol. 58, pp. 93–99, 2 2020.

[6] M. Mozaffari, W. Saad, M. Bennis, Y.-H. Nam, and m. Debbah, "A tutorial on UAVs for wireless networks: Applications, challenges, and open problems," 03 2018.

[7] B. Galkin, J. Kibilda, and L. Dasilva, "A stochastic geometry model of backhaul and user coverage in urban UAV networks," 10 2017.

[8] B. B. H. P. Keeler and M. K. Karray, "SINR-based k-coverage probability in cellular networks with arbitrary shadowing," *Proc. IEEE Int. Symp. Inf. Theory (ISIT)*, pp. 1167–1177, 07 2013.

[9] M. Afshang and H. Dhillon, "Fundamentals of modeling finite wireless networks using binomial point process," *IEEE Transactions on Wireless Communications*, vol. PP, 06 2016.

[10] M. P. et al. "Integrated access and backhaul in 5g mmwave networks: Potential and challenges," *IEEE Communications Magazine*, vol. 58, pp. 62–68, 3 2020.

[11] A. Fouda, A. Ibrahim, I. Guvenc, and M. Ghosh, "UAV-based in-band integrated access and backhaul for 5G communications," 07 2018.

[12] E. Kalantari, M. Z. Shakir, and A. Yongacoglu, "Backhaul-aware robust 3D drone placement in 5G+ wireless networks," 05 2017, pp. 109–114.

[13] C. Pan, J. Yi, C. Yin, J. Yu, and X. Li, "Joint 3D UAV placement and resource allocation in software-defined cellular networks with wireless backhaul," *IEEE Access*, vol. PP, pp. 1–1, 07 2019.

[14] A. Mathai, "An introduction to geometrical probability: Distributional aspects with applications," (*Statistical Distributions and Models with Applications*), vol. 1, 1999.